THE JOURNAL OF BIOLOGICAL CHEMISTRY
Vol. 276, No. 12, Issue of March 23, pp. 9468–9477, 2001
Printed in U.S.A.


# γ-Glutamyltransferase and Its Isoform Mediate an Endoplasmic Reticulum Stress Response*

Received for publication, May 19, 2000, and in revised form, November 29, 2000
Published, JBC Papers in Press, December 14, 2000, DOI 10.1074/jbc.M004352200

**Martin Joyce-Brady‡§¶, Jyh-Chang Jean‡§, and Rebecca P. Hughey§‖**

*From ‡The Pulmonary Center, Boston University School of Medicine, Boston, Massachusetts 02118 and ‖The Laboratory of Epithelial Cell Biology, Department of Medicine, Renal/Electrolyte Division, University of Pittsburgh School of Medicine, Pittsburgh, Pennsylvania 15213*

**Although use of multiple alternative first exons generates unique noncoding 5′-ends for γ-glutamyltransferase (GGT) cDNAs in several species, we show here that alternative splicing events also alter coding exons in mouse GGT to produce at least four protein isoforms. GGTΔ1 introduces CAG four bases upstream of the primary ATG codon and encodes an active GGT heterodimeric ectoenzyme identical to constitutive GGT cDNA but translational efficiency is reduced 2-fold. GGTΔ2–5 deletes the last eight nucleotides of exon 2 through most of exon 5 in-frame, selectively eliminating residues 96–231 from the amphipathic N-terminal subunit, including four N-glycan consensus sites, while leaving the C-terminal hydrophilic subunit intact. GGTΔ7 introduces 22 bases from intron 7 causing a frameshift and a premature stop codon so a truncated polypeptide is encoded terminating with 14 novel residues but retaining the first 339 residues of the native GGT protein. GGTΔ8–9 deletes the terminal four nucleotides of exon 8 plus all of exon 9 and inserts 24 bases from intron 9 in-frame so the C-terminal subunit of the encoded polypeptide loses residues 401–444 but gains eight internal hydrophobic residues. In contrast to the product of GGTΔ1, those derived from GGTΔ2–5, Δ7, Δ8–9 all lack transferase activity and persist as single-chain glycoproteins retained largely in the endoplasmic reticulum as determined by immunofluorescence microscopy and constitutive endoglycosidase H sensitivity in metabolically labeled cells. The developmental-stage plus tissue-specific regulation of the alternative splicing events at GGTΔ7 and GGTΔ8–9 implies unique roles for these GGT protein isoforms. The ability of the GGTΔ1 and GGTΔ7 to mediate the induction of C/EBP homologous protein-10, CHOP-10, and immunoglobulin heavy chain binding protein, BiP, implicates a specific role for these two GGT protein isoforms in the endoplasmic reticulum stress response.**

The entire intron/exon structure of the mouse γ-glutamyltransferase gene (EC 2.3.2.2, GGT)[1] has been defined. This single copy gene is regulated by multiple alternative promoters that are coupled with alternative splicing mechanisms to generate several GGT cDNAs each with a unique 5′-noncoding region. But all encode the same protein, because coding exons appear to be spliced only in a constitutive fashion (1). The protein product is synthesized as a single-chain *N*-glycosylated propeptide, processed into an N-terminal amphipathic subunit and a smaller C-terminal subunit, and expressed on the cell surface where it functions as a key enzyme in glutathione metabolism (2).

Several human GGT cDNAs also exhibit unique 5′-ends and encode a protein that is processed in a similar fashion and shares 79% amino acid identity with that of the mouse (3). In addition, an alternatively processed human GGT cDNA has been described that contains an insertion of 22 bases within the coding domain. The extra nucleotide bases introduce a frameshift and a premature stop codon so that the predicted polypeptide would be a truncated GGT isoform. The protein product has never been characterized, but the elimination of the small subunit suggests that it would lack γ-glutamyltransferase activity. The identification of this alternative transcript implies that human *GGT* gene expression may be more complex than that of other species (4).

However, while characterizing the site of a point mutation in the *GGT*$^{enu1}$ mouse (5), we identified four previously unknown alternative splicing events involving coding exons in the normal mouse *GGT* gene (see Fig. 1). We studied these events to determine whether GGT protein isoforms are being generated through alternative processing of mouse GGT mRNA, to identify if these events are shared between mouse and human GGT, and finally to explore a potential role for these new mouse GGT protein isoforms in glutathione metabolism.

## EXPERIMENTAL PROCEDURES

*Source of Probes and Tissues*—Tri-Reagent (Molecular Research Center, Inc., Cincinnati, OH) was used according to the manufacturer's protocol to isolate total RNA from tissue or cells. Mouse genomic DNA was isolated from the lung. Human genomic DNA was provided by Dr. Qiang Yu from the Pulmonary Center of Boston University. Electrophoresis grade agarose was from International Biotechnologies, Inc. (New Haven, CT), and DNA standards were from Life Technologies, Inc. Materials for protein electrophoresis were from Bio-Rad (Richmond, CA), and protein standards were High-Range molecular weight markers from Amersham Pharmacia Biotech (Piscataway, NJ). X-OMAT and BioMax MR films were used for radiography and obtained from Eastman Kodak Co. (Rochester, NY). [α-$^{32}$P]CTP, specific activity

* This work was supported by National Institutes of Health Grants PO1HL47049 (to M. J. B.) and DK26012 (to R. P. H.) and by the Dialysis Clinic, Inc. The costs of publication of this article were defrayed in part by the payment of page charges. This article must therefore be hereby marked "*advertisement*" in accordance with 18 U.S.C. Section 1734 solely to indicate this fact.

§ These authors contributed equally to this work.

¶ To whom correspondence should be addressed: Tel.: 617-638-4860; Fax: 617-536-8093; E-mail: mjbrady@lung.bumc.bu.edu.

[1] The abbreviations used are: GGT, γ-glutamyltransferase; mGGT, mouse GGT; ER, endoplasmic reticulum; endo H, endoglycosidase H; HBS, HEPES-buffered saline; CHO, Chinese hamster ovary; DMEM, Dulbecco's modified Eagle's medium; Ham's F-12, nutrient mixture Ham's F-12; FBS, fetal bovine serum; CHOP, C/EBP homologous protein-10; BiP, immunoglobulin heavy chain binding protein; hCAR, human coxsackie and adenovirus cell surface receptor; hMUC, human mucin 1; RT, reverse transcription; PCR, polymerase chain reaction; MOPS, 4-morpholinepropanesulfonic acid; PAGE, polyacrylamide gel electrophoresis; kb, kilobase(s); PBS, phosphate-buffered saline.

800 Ci/mmol, was obtained from ICN (Irvine, CA) and [$^{35}$S]Met/Cys, specific activity ~1000 Ci/mmol, was from PerkinElmer Life Sciences (Wilmington, DE) as Easy Tag Express-[$^{35}$S]Protein Labeling Mixture. Primers were synthesized at the DNA/Protein Core Molecular Biology Unit of Boston University School of Medicine. The cDNA probes for CHOP and BiP were generated by PCR after selecting primers based on the published sequences in the GenBank™. The probe for $\beta$-actin has been used routinely in this laboratory. The cell lines hCAR (human coxsackie and adenovirus cell surface receptor) and hMUC (human mucin 1) were available in the laboratory of Dr. Rebecca Hughey (12).

*Genomic PCR, RT-PCR, Subcloning, and Sequencing*—Total RNA from various tissues was used for RT-PCR as described previously (5). PCR primers were selected for primary and secondary PCR reactions, and each PCR reaction was performed for 20 cycles on a MJ Research thermal cycler. PCR products were analyzed by agarose gel electrophoresis, then eluted, cloned into an Invitrogen TA vector (San Diego, CA), and sequenced for verification at the DNA-Protein Core facility at Boston University School of Medicine. RT-PCR primers used for constitutive GGT cDNA amplification were M72, 5′-CCTTTCGGTTTGCCTATGCCAAGAGGAC (upstream); 11M, 5′-GCGCTCCCTCTGTCCCACCCA (nested downstream); and 12M, 5′-GGCTTCCCGCAGCTTGGCGGTGG (primary downstream). For intron 7 and intron 9 insertions, upstream hemi-nested primers were 22U, 5′-GCCAGCTCTGGGGTCTCGGCAG and 24D, 5′-CCTGTCTCCTCCTATGGATCATAG, respectively. The primary primers used for genomic PCR and cloning of intron 7 were M71, 5′-AGGCACTGACGTATCACCGTATCGTG and 10.1M, 5′-CCTCCATCATCCTGAAGGTAGA. Primers M72 plus 10.1M were used in secondary PCR. Intron 9 was cloned using M811, 5′-ACCGCTCACCTGTCTGCGGTTTC as the upstream primer for both PCR reactions together with downstream primers 12M and 11M for primary and secondary PCR, respectively. The relative mRNA abundance of GGTΔ7 *versus* constitutive GGT was determining by using primers 71M plus 11M for the primary reaction, then 72M plus 810M, 5′-GAAACCGCAGACAGGTGAGCGGTGCCTCC, for the secondary reaction.

*Transcription/Translation in Vitro*—TnT T7 Quick-Coupled Transcription/Translation System, a rabbit reticulocyte lysate system, was purchased from Promega and used according to the manufacturer's instructions. Mouse GGT constructs were generated by PCR using upstream primers with (CGGACCGGGCCCTACTGGAAGCAGACCATGAAGA) and without (CGGACCGGGCCCTACTGGAAGACCATGAAGAATC) the CAG insertion 5 bases upstream of the ATG initiation codon along with a common 3′ primer (CCGGAATTCCCGCTGAGTGGGGCACTGGGCACG). Template cDNA was reverse-transcribed from normal mouse kidney mRNA. The 5′ primers contained an *Eco*RI and the 3′ primer an *Apa*I site that were used to clone the PCR products into pCR 2.1 (Invitrogen). Plasmids were sequenced to ensure accuracy, and the T7 promoter was used for *in vitro* transcription. The translated products were labeled with [$^{35}$S]methionine, separated on a 12% polyacrylamide gel, and visualized by autoradiography. The primary translation product was predicted to have a molecular mass of 35.2 kDa with the terminal 47 amino acid residues encoded from the vector. A secondary translation product of 27 kDa was predicted from utilization of an internal translation initiation site.

*Analysis of RNA*—Total RNA was analyzed as previously described (5). RNA obtained from cell lines was quantitated by spectrophotometry and electrophoresed on a 1.0% agarose gel with 2.2 M formaldehyde in 1× MOPS, transferred to a HyBond membrane (Amersham Pharmacia Biotech, Arlington Heights, IL) overnight, both at RT, then cross-linked with a Stratagene UV cross-linker. The membrane was prehybridized with QuickHyb (Stratagene) at 68 °C for 15 min. Radiolabeled probe was then added and incubated for 2 h. The filter was washed twice at room temperature with 2× SSC plus 0.1% SDS, washed twice more with 1× SSC in 0.1% SDS at 60 °C, and dried. An exposure of the filter was made on Kodak X-OMAT film, and the film was developed.

*Stable Expression of mGGT Isoforms in CHO Cells*—A full-length mouse GGT cDNA (type 3) was kindly provided by Drs. Z.-Z. Shi and M. W. Lieberman (Baylor College of Medicine, Houston, TX). This was cloned into the expression vector pCDNA3.1 (Invitrogen). To express the alternatively spliced GGT cDNAs, this wild type GGT cDNA sequence was replaced with that of GGTΔ1, Δ2–5, Δ7 and Δ8–9. All plasmids were sequenced to ensure accuracy.

Plasmids encoding the mGGT isoforms for cell transfections were prepared with the JETstar 2.0 plasmid purification kit (Genomed, PGC Scientifics, Frederick, MD). Stable clonal cell lines were obtained by transfection of Chinese hamster ovary cells (CHO) using LipofectAMINE (1:3 ratio of DNA:lipid; Life Technologies Inc., Gaithersburg, MD) followed by selection in media containing G418 (0.5 mg/ml).

*Transient Expression of mGGT Isoforms in CHO Cells*—Transient expression of the mGGT isoforms was obtained in CHO cells using a cowpox/bacteriophage T7 (vT7CP) expression system as described previously (6, 7). Confluent cultures of CHO cells were grown in 35-mm plastic dishes with a 1:1 mixture of DMEM and Ham's F-12 (1:1) supplemented with 3% FBS (normal culture media). Cells were washed with 1 ml of serum-free medium and infected with vT7CP (multiplicity of infection ~30) in 0.3 ml of the same media for 30 min. The media containing vT7CP was removed from the cells before transfection with a mixture of plasmid DNA (pCDNA3.1 with a T7 promoter) and LipofectAMINE (Life Technologies) at a 1:3 ratio in 1 ml of the same serum-free media for 3 h. The lipid and DNA mixture was them removed, and the cells were washed with 1 ml of DMEM media lacking methionine (Met) and cysteine (Cys) (ICN, Costa Mesa, CA) and returned to culture for 15 min in the same media prior to metabolic labeling.

*Metabolic Labeling of mGGT Isoforms in CHO Cells*—Either stably transfected clonal cell lines expressing the mGGT isoforms or CHO cells transiently expressing the mGGT isoforms (described above) were starved for Met and Cys for 15 min in 1 ml of DMEM media lacking Met and Cys before addition of 50–100 $\mu$Ci of [$^{35}$S]Met/Cys for the times indicated in each experiment. Cells were chased in normal culture medium as indicated. Surface levels of the mGGT isoforms were determined by moving the dishes of cells to ice for biotinylation (8) as previously described (12). Briefly, cells were washed four times with 1 ml of PBS$^{++}$ (137 mM NaCl, 2.6 mM KCl, 15.2 mM $Na_2HPO_4$, 1.47 mM $KH_2PO_4$, 0.5 mM $MgCl_2$ and 0.7 mM $CaCl_2$) then incubated with 0.5 mg/ml sulfo-NHS-SS-biotin (Pierce, Rockford, IL) in triethanolamine-buffered saline (10 mM triethanolamine, pH 7.6, 137 mM NaCl, and 1 mM $CaCl_2$) for 10 min. The reaction was quenched by three washes of the cells with normal culture media. Cells were solubilized as described above, and the supernatants were rotated end over end overnight at 4 °C after addition of protein G immobilized on Sepharose 4B (Sigma Chemical Co., St. Louis, MO) and 1 $\mu$l of goat anti-rat GGT antisera. Immunoprecipitates were recovered by brief centrifugation and washed once with 0.5 ml each of 1% Triton X-100 (Roche Molecular Biochemicals Corp., Indianapolis, IN) in HBS (10 mM HEPES-NaOH, pH 7.4, 150 mM NaCl), 0.01% SDS in HBS and HBS alone. Biotinylated mGGT was recovered by eluting the immunoprecipitates for 2 min at 90 °C in 80 $\mu$l of 1% SDS in HBS and further incubation with 30 $\mu$l of ImmunoPure Immobilized Avidin (Pierce, Rockford, IL) after addition of 0.8 ml of HBS. After overnight rotation at 4 °C, the avidin-conjugated beads were washed with 1 ml each of 1% Triton X-100 in HBS, 0.01% SDS in HBS, and HBS alone. The biotinylated mGGT isoforms were eluted by heating for 3.5 min at 90 °C in 50 $\mu$l of Laemmli SDS-sample buffer containing fresh 0.14 M $\beta$-mercaptoethanol. Samples were subjected to SDS-PAGE on 3–15% polyacrylamide gradient gels, and radioactive protein bands imaged and quantitated from the dried gel using a PhosphorImager (Bio-Rad, Richmond, CA).

*Endoglycosidase H Treatment of Immunoprecipitates*—Radioactive immunoprecipitates were resuspended in 80 $\mu$l of 10 mM citrate buffer, pH 5.0, and 0.5% SDS by heating beads at 90 °C for 2 min (9). The eluted sample was divided in half and incubated overnight at 37 °C with or without 1 milliunit (mU) of endoglycosidase H (endo H, Roche Molecular Biochemicals) in the presence of protease inhibitors (Protease Inhibitor Mixture Set III, Calbiochem, La Jolla, CA).

*Immunofluorescence Microscopy*—COS cells were grown on glass coverslips in 35-mm dishes, transiently transfected with the cDNAs for the mGGT isoforms using LipofectAMINE, and analyzed by immunofluorescence 2 days later. All steps were carried out at room temperature. Cells were washed once with PBS$^{++}$ for 5 min prior to fixation with 3% paraformaldehyde in PBS$^{++}$ for 12 min. After washing with 10 mM glycine in PBS$^{++}$ (PBS-Gly), cells were permeabilized by incubation for 4 min in 0.5% Triton X-100 in PBS-Gly and blocked with 5% goat serum in PBS-Gly for 5 min. Cells were incubated with rabbit anti-rat GGT antisera (diluted 1/600) for 45 min and then CY3-conjugated goat anti-rabbit IgG (diluted 1/2500; Jackson ImmunoResearch Laboratories, Inc., West Grove, PA) for 30 min, both in 1% goat serum in PBS-Gly. Cells were incubated for 5 min with 0.5 $\mu$g/ml 4′-6-diamidino-2-phenylindole (Molecular Probes, Eugene, OR) in PBS-Gly to stain nuclei and then washed twice for 5 min with PBS-Gly before mounting on slides with 1 M *n*-propylgallate in glycerol and viewing with a Nikon Optiphot-2 microscope. Calnexin was stained as a positive control for localization in the endoplasmic reticulum (ER) using an antibody directed against the cytosolic tail (StressGen Biotechnologies Corp., Victoria, Canada).

*Enzyme Activity*—Specific GGT enzyme activity was measured at room temperature using the substrates $\gamma$-glutamyl-para-nitroanilide

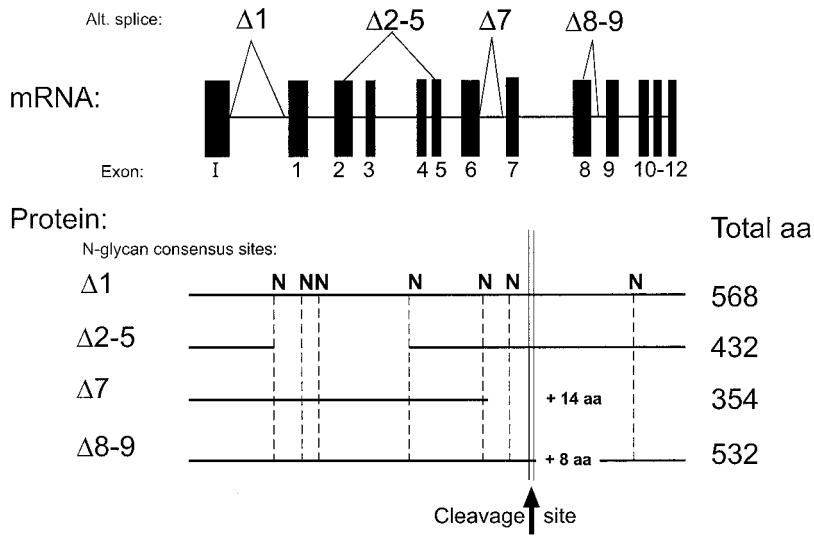


FIG. 1. **Alternative splicing events in mouse GGT.** This schematic depicts the constitutive (*1*) and the alternative (Δ) splicing events of mouse GGT mRNA and the protein isoforms that result based on data in Table I and Figs. 2–8.

and glycylglycine as previously described (10). Protein was determined by the method of Lowry.

## RESULTS

*Mouse GGTΔ1*—The majority of our PCR-derived GGT clones generated from lung and kidney RNA of wild type and *GGT*$^{enu1}$ mice contained the trinucleotide insert CAG five bases upstream of the ATG initiation codon (details in Fig. 1). An examination of GGT cDNA sequences in the GenBank™ revealed an absence of this CAG insert in all mouse GGT cDNAs, as well as those from rat and pig, but revealed its presence in most, but not all, human GGT cDNAs. Certain human lung GGT cDNAs lacked this CAG insert (11). Because this CAG insertion is located at an intron/exon junction, we compared the intron sequences from the mouse, rat, and pig to determine whether alternative splicing could account for its presence (Fig. 2*A*). All three introns contain the highly conserved dinucleotides GT and AG at the 5′- and 3′-boundaries, respectively, and the AG is preceded by a cytosine residue. However, the mouse intron contains two CAGs in tandem at its 3′-intron boundary, whereas the rat and the pig intron each contain a single CAG. We then cloned and partially sequenced a corresponding human GGT intron sequence. We confirmed that this intron is identical in size to that of rat, mouse, and pig, ~0.5 kb, and contains two tandem CAG trinucleotides at the 3′-boundary like that of mouse.

To see if the proximity of this CAG insert to the ATG initiation site could affect the site of translation initiation, we used a transient VT7CP expression system to characterize the protein encoded by the GGTΔ1. Cow pox-infected CHO cells transfected with the GGTΔ1 plasmid were starved for Met and Cys and pulse-labeled in the same media with [$^{35}$S]Met/Cys, before a chase period of 0 or 2 h. SDS-PAGE analysis of GGT-specific immunoprecipitates from the cell extracts revealed a single peptide of 83 kDa at $t = 0$, which was sensitive to treatment with endoglycosidase H and produced a product of 59 kDa (Fig. 3), consistent with expression of the full-length propeptide of 61 kDa (Table I). Because endo H removes all but one GlcNAc residue of high mannose *N*-glycans ($M_r$ ~ 3000) from glycoproteins, this difference in $M_r$ (2400) is consistent with *N*-linked glycosylation of the GGTΔ1 at all seven consensus sites (Asn-*X*-Ser/Thr). After 2 h of chase, only a trace of the 83-kDa propeptide was evident, whereas the two expected subunits of the cleaved GGT propeptide were present at 50 and 23 kDa. Endo H treatment of this sample produced trace bands at 33 and 20 kDa, consistent with the presence of six *N*-glycans and one *N*-glycan on the subunits, respectively. The more diffuse

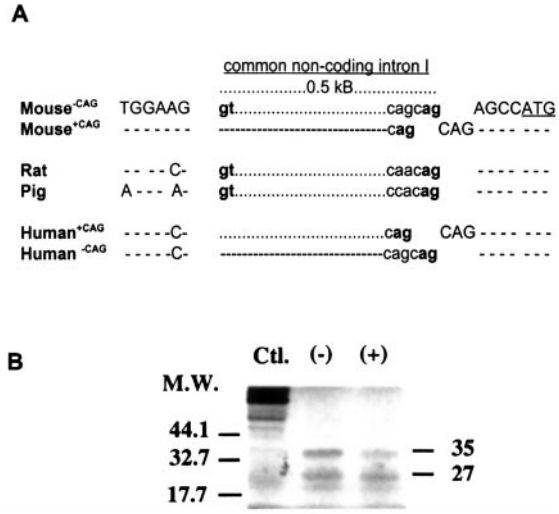


FIG. 2. **Characterization of GGTΔ1.** *A*, comparison of nucleotide sequences at the intron boundary between mouse, rat, pig, and human GGT. *Uppercase letters* are cDNA, and *lowercase letters* are intron sequences. Dinucleotides at intron boundary are in *boldface*. *B*, an *in vitro* transcription/translation assay as described under "Experimental Procedures" using constructs which lack (−) or contain (+) the CAG insertion as seen in constitutive mGGT or GGTΔ1, respectively. Molecular weight markers (*M.W.*) are shown to the *left* of the internal positive control (*Ctl.*). The primary translation product is marked at 35 kDa. The translation product from an internal initiation site is marked at 27 kDa.

gel pattern of the large subunit indicated that there is considerable microheterogeneity in the processing of these *N*-glycans, whereas the small subunit was more homogeneous despite its resistance to endo H treatment, indicating that the single *N*-glycan is minimally processed.

Similar data were obtained for the synthesis of GGTΔ1 in stable transfectants of CHO cells (Fig. 4). When these clonal CHO cells expressing GGTΔ1 were pulse labeled for 30 min and chased for 2 h prior to cell surface biotinylation with the membrane impermeant sulfo-NHS-SS-biotin, ~20% of the heterodimer was recovered from the immunoprecipitates with avidin-conjugated beads. This indicated that the GGTΔ1 protein did reach the plasma membrane (compare *mock lanes* in Fig. 4, *A* and *B*). This cell surface localization of the GGTΔ1 was confirmed by immunofluorescence analysis of COS cells 2 days after transfection with the GGTΔ1 cDNA (Fig. 5*A*). A similar pattern of immunofluorescence was observed in stably trans-

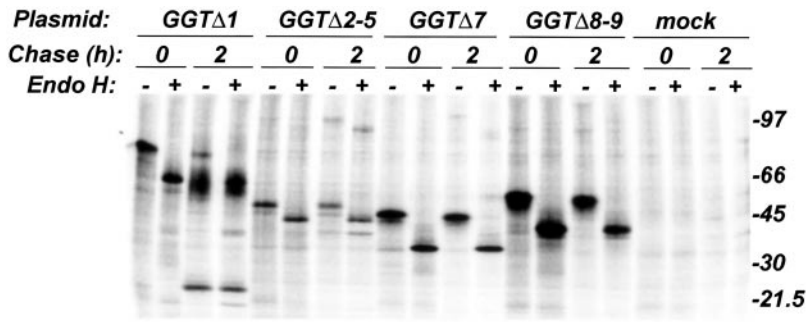


FIG. 3. **Transient expression of mouse GGT isoforms in CHO cells.** Confluent cultures of CHO cells in 35-mm wells were infected with cow pox for 30 min before transfection for 2 h with 18 $\mu$g of LipofectAMINE and either no plasmid (*mock*) or 6 $\mu$g of plasmid DNA encoding GGTΔ1, GGTΔ2–5, GGTΔ7, or GGTΔ8–9. Cells were pulse-labeled for 15 min with [$^{35}$S]Met/Cys prior to chase periods of 0 or 2 h, before extraction with octyl glucoside and immunoprecipitation of the GGT-related peptides with a goat polyclonal antibody and subsequent treatment overnight with (+) or without (−) endo H. Samples were subjected to SDS-PAGE and PhosphorImager analysis. *Numbers* to the *right* refer to the mobility of molecular mass standards in kDa.

TABLE I
*Characteristics of mouse GGT protein isoforms*

| mGGT isoform | Peptide FW[a] | *N*-Glycan consensus site[b] | SDS gel $M_r$ (± end H)[c] | $M_r$ difference[d] | No. of *N*-Glycans estimated[e] | Half-life[f] (CHO clone/ VT7CP) |
|---|---|---|---|---|---|---|
| Δ1 | 61.2 | 7 | 78/59 | 24 | 7 | 18.7/17.4 |
| Δ2–5 | 46.7 | 3 | 47/38 | 9 | 3 | 1.7/2.1 |
| Δ7 | 38.2 | 5 | 44/32 | 12 | 4 | 6.5/10.2 |
| Δ8–9 | 57.6 | 7 | 52/37 | 15 | 5 | ND/0.9 |

[a] Formula weight was calculated from the predicted amino acid sequence.
[b] The consensus sequence for *N*-linked glycosylation is Asn-*X*-Ser/Thr.
[c] Apparent molecular weight of isoform on SDS gel as shown in Fig. 4.
[d] Difference in molecular weight of the isoform before and after treatment with endo H.
[e] Calculated number of *N*-linked glycans, assuming that removal of each glycan alters mobility by 3 kDa.
[f] Half-life was calculated from recover of [$^{35}$S]GGT isoforms after chase times of 3 and 18 h (Δ1 and Δ7) or chase times of 0 and 3 h (Δ2–5 and Δ8–9) as described under "Experimental Procedures." A clonal CHO cell line expressing Δ8–9 was not available.

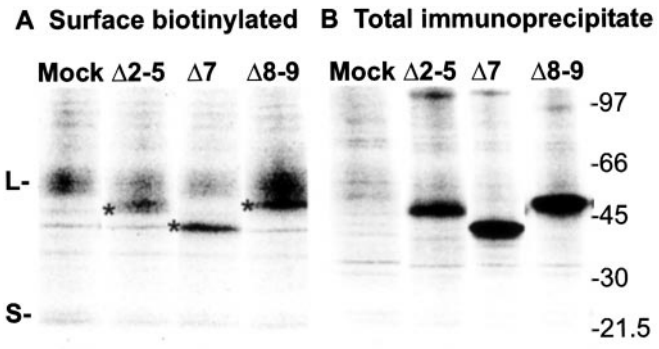


FIG. 4. **Only GGTΔ1 is expressed at the cell surface.** Confluent cultures of clonal CHO cells stably expressing the GGTΔ1 in 21-mm wells were infected with cow pox for 30 min before transfection with 9 $\mu$g of plasmid DNA encoding GGTΔ2–5, GGTΔ7, or GGTΔ8–9 (*mock* received buffer and no DNA). The next day, cells were pulse-labeled for 30 min with [$^{35}$S]Met/Cys prior to a 2-h chase period, before biotinylation of the cell surface on ice, extraction with octyl glucoside, and immunoprecipitation of the GGT. A portion of the immunoprecipitate (75%) was further incubated with avidin-conjugated beads to obtain the biotinylated cell surface GGT. Both a portion of the total immunoprecipitate (*B*, 25% of total) and the biotinylated surface GGT (*A*) were subjected to SDS-PAGE and PhosphorImager analysis. *Numbers* to the *right* refer to the mobility of molecular mass standards in kDa. The mobility of the large (*L*) and small (*S*) subunits of the GGTΔ1 heterodimer are shown on the *left*, and the *asterisk* indicates protein isoforms. The diffuse gel pattern of the GGTΔ1 large subunit indicates that there is considerable microheterogeneity in the processing of the *N*-glycans. This band is less evident in *B*, because these *lanes* represent only 25% of each immunoprecipitate.

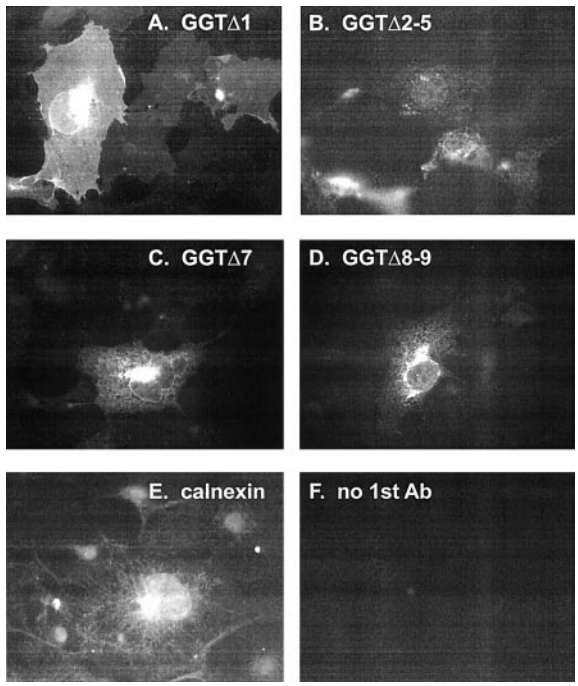


FIG. 5. **Immunofluorescence analysis.** COS cells were transfected with plasmids encoding GGTΔ1 (*A*), Δ2–5 (*B*), Δ7 (*C*), and Δ8–9 (*D*). The steady-state localization of the expressed proteins were analyzed with rabbit anti-rat GGT antiserum followed by fluorescein isothiocyanate-labeled goat anti-rabbit IgG. COS cells (*E*) were stained for calnexin as a positive control for an ER protein, and primary antibody was omitted for a negative control (*F*). Surface staining is observed only for mGGTΔ1. Although Δ2–5, Δ7, and Δ8–9 predominantly show staining in the endoplasmic reticulum, a low level of juxtanuclear Golgi-like staining is also seen for all the proteins.

fected CHO cells expressing the GGTΔ1 (data not shown). In both cases nearly all the GGT-specific immunofluorescence was found at the cell surface. An equally important result is that the clonal CHO cells expressing GGTΔ1 exhibited a much higher γ-glutamyl transferase-specific enzymatic activity (280

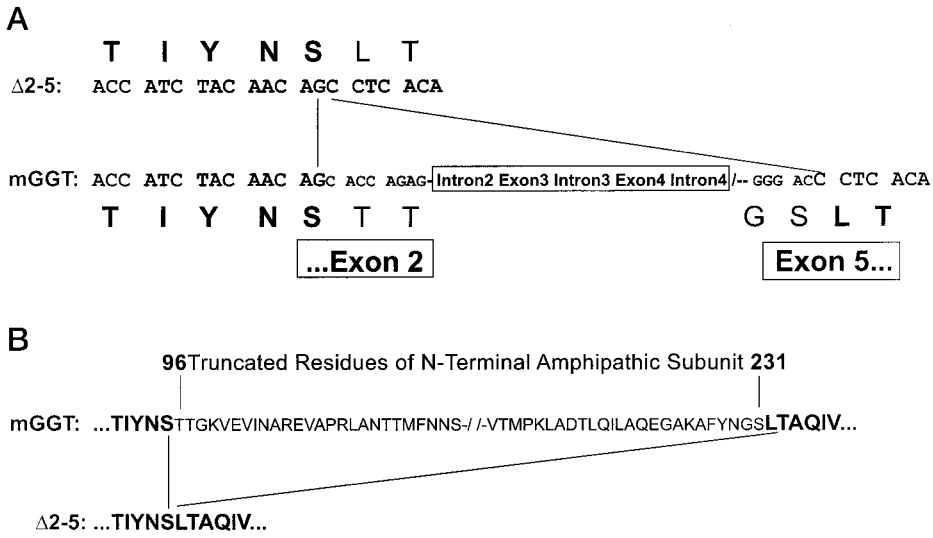


FIG. 6. **Characterization of GGTΔ2–5.** *A*, an event resulting from usage of 5′- and 3′-splice sites within exon 2 and exon 5, respectively. The last eight nucleotides of exon 2, all of exons 3 and 4, and most of exon 5 are eliminated. *B*, the encoded protein loses amino acid residues 96 through 231, including four *N*-glycan consensus sites from the amphipathic N-terminal subunit, whereas the C-terminal hydrophilic subunit remains intact.

mU/mg) than nontransfected CHO cells (<1 mU/mg). And after overnight accumulation of GGTΔ1 in transfected cow pox-infected CHO cells, this enzyme activity was greatly increased (200–1000 mU/mg). Because this latter result indicated that the GGTΔ1 protein must be relatively stable, the half-life was determined for the radiolabeled GGTΔ1 during stable and transient expression by pulse-labeling cells for 30 min and immunoprecipitating GGTΔ1 after chase times of 3 and 18 h (Table I). Calculation of the half-life from the percent loss of radiolabeled GGT between the two time points indicated the half-life for the GGTΔ1 is similar in stable (18.7 h) and transiently transfected (17.4 h) CHO cells. Thus GGTΔ1 encodes the normal mouse GGT protein. This protein exhibited normal synthesis, cell surface expression, stability, and enzymatic activity. Because the expression of GGTΔ1 in cultured cells was indistinguishable from that described previously for rat and human GGT, we next assessed whether the CAG insert in the mouse GGTΔ1 could affect translational efficiency using an *in vitro* transcription/translation assay. The synthesis of the primary translation product (35.2 kDa) from the transcript containing the CAG insert was reduced ~2-fold when compared with synthesis from a transcript lacking the CAG sequence, whereas synthesis of an alternate protein from an internal ATG codon (27 kDa) was unchanged (Fig. 2*B*). Thus, the CAG appears to regulate translation of the GGT mRNA, not the protein product.

*Mouse GGTΔ2–5*—This alternative splicing event produces an in-frame deletion of the last eight nucleotides of exon 2, all of exons 3 and 4, and most of exon 5 (Fig. 6*A*). Nonconsensus 5′- and 3′-splice sites appear to have been utilized in exons 2 and 5, respectively. We could not identify a corresponding human GGT mRNA transcript but did find at least two alternative rat GGT cDNAs using mRNA from cultured rat alveolar type 2 cells that utilized the same 5′-splice site (data not shown). The encoded protein loses amino acid residues 96 through 231, including four *N*-glycan consensus sites from the amphipathic N-terminal subunit, while the C-terminal hydrophilic subunit remains intact (Fig. 6*B*).

When CHO cells transiently transfected with the GGTΔ2–5 were pulse-labeled with [$^{35}$S]Met/Cys for 15 min, a single labeled protein of 47 kDa was immunoprecipitated after both 0- and 2-h chases (Fig. 3). At both time points the protein was sensitive to endo H treatment producing a protein of 38 kDa, consistent with the presence of three *N*-glycans, but which is notably smaller than the predicted sequence (46.7 kDa). Because the protein remains anchored to the membrane (data not shown), this indicates that the GGTΔ2–5 either is cleaved after the *N*-glycan consensus site in the small subunit or migrates anomalously on SDS gels.

The persistence of the endo H sensitivity of the GGTΔ2–5 protein after the 2-h chase also suggests that the protein is retained in the ER or early Golgi rather than moving to the cell surface. When this was tested by transient expression of GGTΔ2–5 in CHO-GGTΔ1 cells, only 1.5% of the GGTΔ2–5 was biotinylated at the cell surface after a 2-h chase, whereas ~20% of the GGTΔ1 was biotinylated in the same cells (Fig. 4). Localization in the ER was also evident by immunofluorescence microscopy of COS cells transiently expressing the GGTΔ2–5 (Fig. 5*B*). Determination of the half-life for the GGTΔ2–5 in both stable transfected (1.7 h) and transiently transfected (2.1 h) CHO cells indicates that this isoform of the mouse GGT is considerably less stable than the GGTΔ1 (Table I). Enzyme assays of these cell extracts reveal no increase in γ-glutamyltransferase activity (<1 mU/mg) above the control levels observed in nontransfected CHO cells.

*Mouse GGTΔ7*—This alternative splicing event introduces a 22-base insertion within the coding domain. This insertion mimics that in humans and induces a frameshift and a premature stop codon within the open reading frame (Fig. 7*A*). The encoded mouse protein is a truncated GGT-like protein that retains only the first 339 amino acids of the native GGT protein and gains 14 novel residues at the C terminus, the first seven of which are identical to that in the human (Fig. 7*B*). Because the intron/exon structure of mouse GGT is known and the last 10 nucleotides at the 3′ terminus of the insert agree exactly with the intron 7 sequences in the literature (1), it appears that the 22-base insertion results from an alternative splice site at intron 7. To confirm this, we cloned and partially sequenced the ~3 kb of mouse intron 7 (Fig. 7*A*). The remaining 10 nucleotides at the 5′-end of the insertion were identified as intron 7 sequences, and they were preceded by a CAG as a 3′-splice site. This 22-base mouse intron sequence is identical to the corresponding human intron sequence (Fig. 7*C*).

We used the 22-base insert as one of the primers in a PCR reaction to determine whether the GGTΔ7 splicing event is regulated in a developmental or tissue-specific fashion. We analyzed heart, liver, lung, kidney, and thymus RNA obtained from 1-day-old and adult mice (Fig. 7*D*). We detected GGTΔ7 in the RNA from the heart but not that from the liver or the lung during the neonatal period. RNA from the adult lung served as a positive PCR control here. In adult tissues, GGTΔ7 was present in RNA from the lung, the kidney, and the thymus but

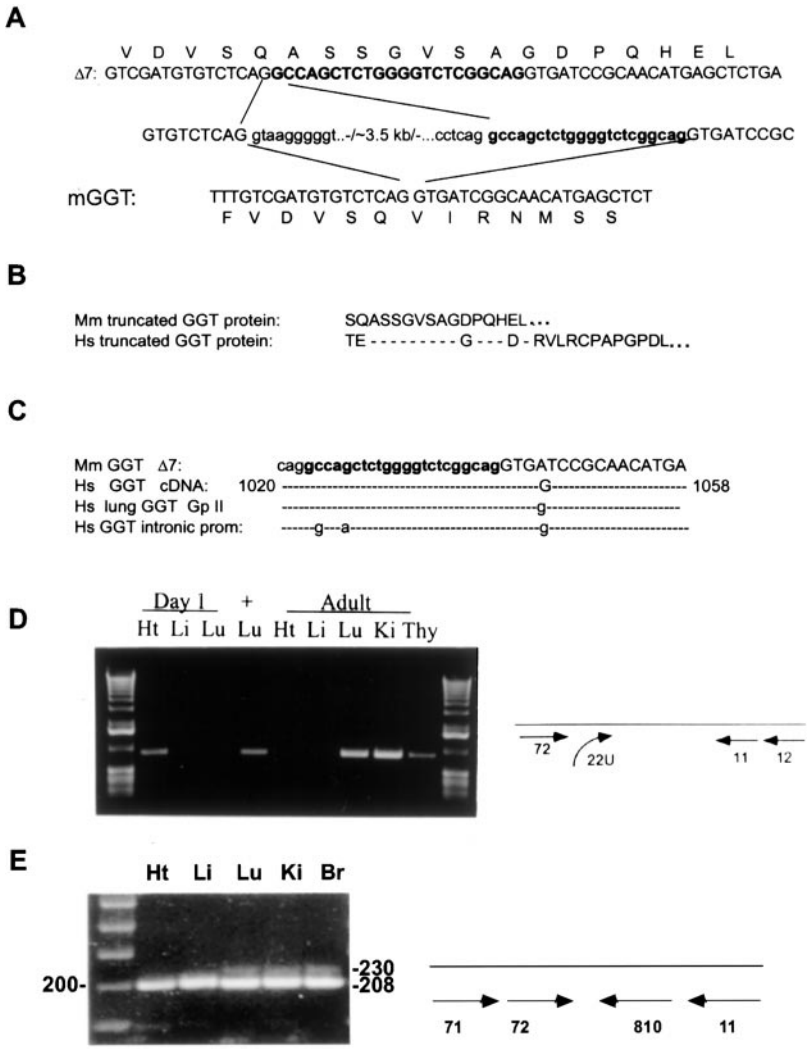


FIG. 7. **Characterization of GGTΔ7.** *A*, as a result of this event, 22 bases are inserted (*boldfaced*) into the mouse Δ7 cDNA, and this alters the reading frame from that of mGGT cDNA. *B*, a truncated mouse GGT protein (*Mm*) is encoded with a new C terminus that is similar to that predicted from an alternatively processed human GGT cDNA (*Hs*). *C*, this 22-base insertion in mouse GGT cDNA is identical to that described in human GGT cDNA and human lung-specific group II GGT cDNAs (*Gp II*) and very similar to sequences of a human GGT intronic promoter. *D*, PCR analysis as described under "Experimental Procedures" with primer 22U shows that this alternative splicing event is detectable in newborn mouse heart (*Ht*) but not liver (*Li*) nor lung (*Lu*). Adult lung (+) was amplified with constitutive primers to serve as the positive control in this PCR reaction. In a separate PCR reaction for adult tissues, GGTΔ7 is undetectable in heart (*Ht*) and liver (*Li*) but evident in lung (*Lu*), kidney (*Ki*), and thymus (*Thy*). *E*, a PCR analysis was also performed as described under "Experimental Procedures" to compare the relative abundance of GGTΔ7 (230-bp product) *versus* constitutive mGGT (208-bp product) in heart (*Ht*), liver (*Li*), lung (*Lu*), kidney (*Ki*), and brain (*Br*).

absent from that of the heart and the liver. It was also detectable in mRNA isolated from adult rat kidney and human peripheral blood mononuclear cells (data not shown).

To compare the relative abundance of GGTΔ7 to constitutive mGGT, we amplified the mRNAs from five different tissues using two sets of PCR primers that were common to both transcripts with a fully nested design (Fig. 7*E*). The 208-base pair signal amplified from constitutive mGGT was evident in all samples. The 230-base pair signal amplified from GGTΔ7 was only evident in lung, kidney, and brain and was less abundant than that of the constitutive GGT signal.

When CHO cells transiently expressing the GGTΔ7 were pulse-labeled for 15 min with [$^{35}$S]Met/Cys a single product of 44 kDa was obtained after chase times of both 0 and 2 h (Fig. 3). Endo H treatment produced a peptide of 32 kDa in both cases, which was slightly smaller than the peptide size calculated from the predicted sequence (38.2 kDa), but indicates that *N*-glycans are present at four of the five consensus sites in the GGTΔ7. When the cell surface of CHO-GGTΔ1 cells transiently expressing the GGTΔ7 were biotinylated after a 30-min pulse with [$^{35}$S]Met/Cys and a 2-h chase, only 0.5% of the GGTΔ7 was recovered with avidin-conjugated beads while 37% of the GGTΔ1 was recovered from the same cells (Fig. 4). Immunofluorescence microscopy of COS cells transiently expressing the GGTΔ7 (Fig. 5*C*) revealed staining of the ER, which is consistent with both the persistence of endo H sensitivity and the minimal cell surface expression of this isoform. Enzyme assays for both CHO cells stably and transiently expressing GGTΔ7 revealed no increase in γ-glutamyltransferase activity (<1 mU/mg) above the control levels observed in nontransfected CHO cells. The half-life for the GGTΔ7 in these same cells (6.5 and 10.2 h, respectively) was approximately half of that observed for the GGTΔ1 (Table I).

*Mouse GGTΔ8–9*—The Δ8–9 alternative splicing event eliminates at least the last four nucleotides of exon 8 and all of exon 9 but introduces 24 novel bases (Fig. 8*A*). The last 10 of these 24 nucleotides are identical to the published sequence at the 3′-boundary of intron 9 (1). This intron was cloned and sequenced, and the remaining 14 nucleotides were confirmed as intron 9 sequences, which were preceded by a CAG sequence. If this CAG represents the 3′-intron boundary, then the 5′-splice site lies within exon 8 but it is a nonconsensus splice site. However, other nonconsensus dinucleotide sequences could also border these boundaries as denoted in Fig. 8*A*, so the exact location of this splice site is unclear. This GGT cDNA has not been described in humans and we did not detect any PCR product when this 24-base insert was used as a PCR primer with human cDNA (data not shown). To confirm this, we cloned and sequenced a corresponding human intron. The 67 nucleotides at the 3′-boundary of our clone matched perfectly with sequences in human *GGT* genes 3, 6, and 11 (data not shown). However, comparison with mouse intron 9 revealed neither conserved sequences in this region nor any conserved 3′-splice site sequences (Fig. 8*B*). Usage of the 24 corresponding human nucleotides also failed to produce a PCR product. Hence, this particular GGT splicing event may be specific to mouse.

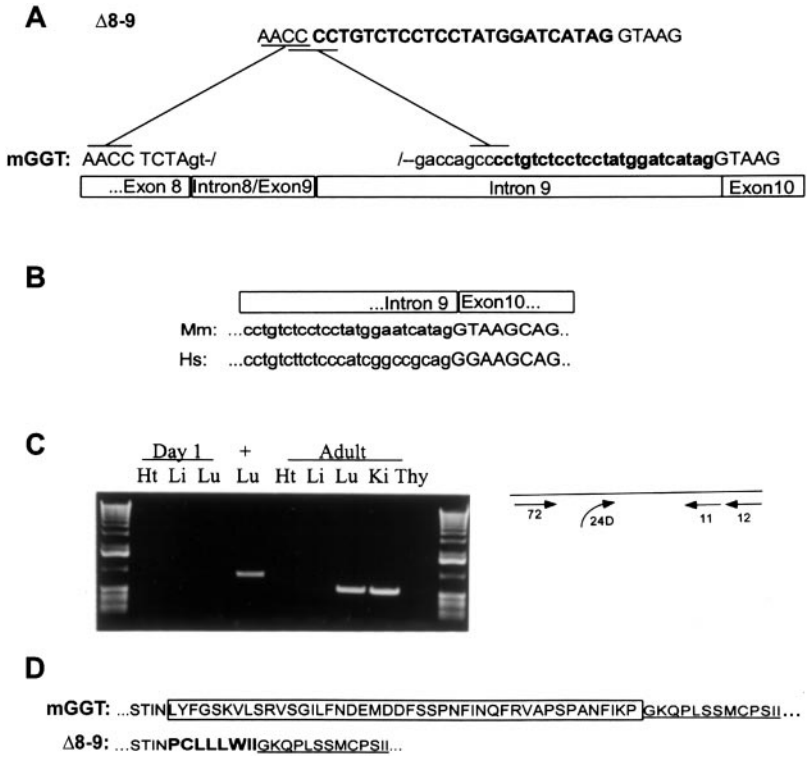


FIG. 8. **Characterization of GGTΔ8–9.** *A*, this exact site of the splicing event for Δ8–9 is unclear but appears to involve alternative nonconsensus 5′- and 3′-splice sites within exon 8 and intron 9, respectively. The last four nucleotides of exon 8 are eliminated, and 24 bases from intron 9 (*boldfaced*) are inserted into the GGTΔ8–9 cDNA. *B*, comparison of the terminal 25 nucleotides from mouse (*Mm*) intron 9 with those from the corresponding human (*Hs*) intron reveals many differences. *C*, PCR analysis for developmental and tissue-specific expression of Δ8–9 was performed as in Fig. 7, but the upstream primer in the secondary PCR reaction was 24D. *D*, the amino acid residues that are eliminated from the small C-terminal subunit of mGGT are *boxed*, and the eight novel amino acids of Δ8–9 are *boldfaced*. These hydrophobic residues are inserted proximal to the active enzyme site of mGGT (*underlined*).

To determine if Δ8–9 was expressed in a developmental or tissue-specific fashion, we repeated the analysis outlined for GGTΔ7 but used the 24-base insert as one PCR primer. GGTΔ8–9 was not detected in RNA from the heart, the liver, or the lung during the neonatal period, even though it was present in the adult lung-positive control. In adult tissues, it was evident in RNA from the lung and the kidney but not that from the heart, the liver, or the thymus (Fig. 8*C*). Hence, GGTΔ8–9 exhibits developmental-stage and tissue-specific regulation, but the patterns differ from that of GGTΔ7.

The elimination of the terminal four bases of exon 8 plus all of exon 9 together with the insertion of 24 bases from intron 9 removes 44 amino acids residues from the C-terminal small subunit but adds 8 novel amino acids proximal to active enzyme site residues (Fig. 8*D*). When CHO cells transiently transfected with the GGTΔ8–9 were pulse-labeled with [$^{35}$S]Met/Cys for 15 min, a single labeled protein of 52 kDa was immunoprecipitated after both 0- and 2-h chases (Fig. 3). At both time points the band was sensitive to endo H treatment producing a protein of 37 kDa, consistent with the presence of five *N*-glycans on the protein. However, this is two less *N*-glycans than would be predicted from the GGTΔ8–9 sequence. In addition, the protein size for the GGTΔ8–9 calculated from the predicted sequence is considerably larger (57.6 kDa). The cumulative data would be most consistent with cleavage of the GGTΔ8–9 into an unstable heterodimer, immediate degradation of the small subunit, and retention of the residual large subunit within the ER. When the cell surface of CHO-GGTΔ1 cells transiently expressing the GGTΔ8–9 were biotinylated after a 30-min pulse with [$^{35}$S]Met/Cys and a 2-h chase, only 2.2% of the GGTΔ8–9 was recovered with avidin-conjugated beads while 35% of the GGTΔ1 was recovered from the same cells (Fig. 4). Immunofluorescence microscopy of COS cells transiently expressing the GGTΔ8–9 (Fig. 5*D*) revealed staining of the ER, which is consistent with both the persistence of endo H sensitivity and the poor cell surface expression of this isoform. The half-life of the GGTΔ8–9 in transiently transfected cells was only 0.9 h, and there was no measurable γ-glutamyltransferase enzymatic activity. Although stably transfected cells were not available for these studies, the similar data obtained for the GGTΔ1, GGTΔ2–5, and GGTΔ7 between transient and stably transfected cells (Table I) indicates that the half-life and the enzyme activity data for GGTΔ8–9 in transiently transfected cells are reliable.

*Stress Response Induction in the Endoplasmic Reticulum*—Because GGTΔ1 is normally found at the cell surface, the localization of the GGTΔ2–5, Δ7, and Δ8–9 in the ER could simply indicate that these GGT isoforms are abnormally folded products and they are being retained for subsequent degradation. Alternatively, this subcellular localization could be consistent with a new previously undefined role for these proteins within the ER. The active GGTΔ1 enzyme is essential for turnover of glutathione at the cell surface. Although the other GGT isoforms lack this enzyme activity, they could still bind substrate and act as sensors of the critical glutathione redox levels found in ER. In support of this hypothesis, we found that the phenotype of the stable CHO cells for GGTΔ1 and Δ7 changed dramatically when the cell media was shifted from a 1:1 mixture of DMEM (cystine) and Ham's F-12 (cysteine) with 3% FBS to DMEM alone with 3% FBS. Although the GGTΔ2–5 and Δ8–9 cells remained unchanged, the GGTΔ1 and Δ7 cells rounded, lifted, and detached from the culture plates within 12 h. The altered phenotype was reversed upon return of the cells to the original media containing cysteine as well as cystine. Because stress in the ER can be associated with this dramatic change in phenotype, we probed the cellular RNA from each cell line for the induction of CHOP-10 and BiP mRNAs, two markers of the ER stress response. CHOP-10 mRNA was not detected by Northern blot analysis in any of the cell lines before the change in media (data not shown) but was dramatically induced in the GGTΔ1 and Δ7, but not the GGTΔ2–5 and Δ8–9 cells, during the recovery period (Fig. 9). Actin mRNA was examined as a control for RNA loading and integrity and was unchanged. To be sure this induction of CHOP-10 was not due simply to overexpression of a recombinant protein, two additional cell lines expressing high levels of

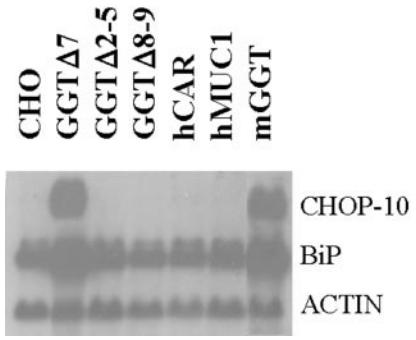


FIG. 9. **Expression of GGTΔ1 and Δ7 mediate the ER stress response in CHO cells.** Control nontransfected CHO cells, and CHO expressing GGTΔ1, Δ2–5, Δ7 or Δ8–9, or the recombinant control proteins hCAR or hMUC1 were maintained in DMEM/Ham's F-12 with 3% FBS. The media was changed to DMEM alone with 3% FBS for 12 h, and RNA was extracted from cells after 7 days recovery in DMEM/Ham's F-12 with 3% FBS. RNA was analyzed by filter hybridization as described under "Experimental Procedures" using CHOP-1, BiP, and β-actin probes. No signal for CHOP-10 was evident in cells at baseline.

the recombinant glycoproteins hCAR or MUC1 (12) were similarly characterized and found to not induce CHOP in response to the change in media. Although hCAR is a 46-kDa glycoprotein cell surface receptor for coxsackie and adenoviruses (13), MUC1 is a very heavily *O*-glycosylated mucin-like transmembrane protein ($M_r$ > 220 kDa (12)). Finally, analysis of BiP mRNA levels in all these cell lines indicated that its expression paralleled that of CHOP-10.

## DISCUSSION

Herein we have characterized four new GGT protein isoforms that are derived from alternative splicing events in mouse GGT cDNA. The mouse and the human not only generate GGT protein isoforms by this mechanism, but they share some of these splicing events in common. The encoded GGT protein isoforms can be expressed as transferase active heterodimeric glycoproteins on the cell surface or as transferase inactive monomeric glycoproteins in the endoplasmic reticulum. These latter findings suggest potentially novel functions for native GGT protein and its protein isoforms within the endoplasmic reticulum in addition to the known role of the native protein as a cell surface ectoenzyme.

Alternative pre-mRNA splicing of nascent eukaryotic mRNAs is a post-transcriptional process that is known to be highly regulated and widely utilized to generate multiple alternative products from a single gene (14). A prime example of the power of alternative promoters to generate such mRNA diversity can be found in the mouse *GGT* gene itself. Six GGT cDNAs, each with a unique 5′-untranslated region, are generated from this single copy gene via six alternative promoters (15). Alternative splicing events within the open reading frame can generate protein isoforms by excluding specific exon sequences or including novel intron sequences in the mature mRNA transcript. However, prior to our study, only a constitutive splicing pattern had been identified in the mouse *GGT* gene, which involves the invariant ligation of 12 coding exons, numbered by *Arabic numerals 1* through *12*, and one common noncoding exon, numbered by *Roman numeral I* as depicted in Fig. 1 (1).

The central difference between constitutive and alternative splicing lies in the selection and ligation of specific pairs of donor/acceptor splice sites. This is a complex process that is only partially understood, but it is clear that certain *cis* RNA sequences provide recognition sites for *trans*-splicing factors that form the spliceosome apparatus. These *cis* RNA sequences include the dinucleotides GT and AG located at the 5′- and the 3′-boundaries of an intron, respectively (16). These conserved dinucleotide sequences are found at all of the intron boundaries in the constitutively spliced mouse *GGT* gene (1). The factors involved in the selection of these specific GT and AG residues from a much large number of potential choices are not yet fully known for any gene. However, additional consensus sequences surrounding these dinucleotides as well as internal consensus sequences at the branch point participate in the selection process. Selection of the AG residue at the 3′-splice site appears to involve a scanning process initiated from the branch point and a competition among various intervening AG dinucleotides with the nucleotide preceding the AG having a profound influence on its selection in the order CAG~TAG > AAG > GAG (16). In GGTΔ1 and GGTΔ7 the alternative splicing event was limited to the 3′-intron boundary and utilized an alternative AG dinucleotide that was preceded by a cytosine residue. In GGTΔ2–5 and GGTΔ8–9 the alternative splicing events involved 5′- and 3′-splice sites as well as non-GT/AG dinucleotides.

In GGTΔ1 two CAGs in tandem are present at the 3′-boundaries of the corresponding introns in mouse and human GGT but absent from those of the rat and the pig. Our results show that alternative utilization of these sites can explain the presence or absence of a CAG trinucleotide insert upstream of the ATG initiation codon specifically in mouse and human GGT cDNAs. The scanning model predicts that the first CAG should identify the 3′-boundary of the intron while the second should be present in the cDNA. Our data agrees with this model, because 80% of the clones contained the CAG insertion. Despite the proximity of these bases to the translation initiation site, our protein expression studies clearly show that the heterodimer derived from GGTΔ1 is a stable protein and identical to that described previously in the rat and in humans (9, 17). Hence, the mouse and humans express two GGT cDNAs that encode a GGT propeptide, which is heavily glycosylated, especially on the large subunit, and processed into the heterodimer before or after delivery to the cell surface. Our study now represents the first detailed characterization of the GGT glycoprotein in the mouse. The activity associated with this enzyme initiates the hydrolysis of reduced or oxidized glutathione at the cell surface, a process that is essential for recovery and uptake of cysteine/cystine. However, this metabolism also appears to generate the pro-oxidant hydrogen peroxide in the presence of iron (18). Hence, it is likely that the level of GGT activity is regulated. Our *in vitro* transcription/translation data shows that mouse and human GGT can use the insertion of this CAG sequence to down-regulate GGT protein production at the level of translation. The utilization of this same alternative splicing strategy to alter mRNA translational efficiency has already been described in the gene for human surfactant-associated protein A2, so it is not unique to GGT (19, 20).

GGTΔ7 also utilizes a nearby AG dinucleotide located only 24 bases pairs upstream in intron 7 as the alternative 3′-intron boundary, and this is preceded by a cytosine residue. Two factors could have selected against this CAG as the constitutive 3′-splice site according to the scanning hypothesis. The first is a distance of less than 12 nucleotides from the branch point; the second is a location within a region of secondary mRNA structure such as stem loop. Our partial sequence analysis of mouse intron 7 supports the first mechanism. We found that there is a potential branch point consensus sequence that would place this alternative CAG within this distance restriction. There is also a second potential branch point sequence even further upstream that would also place it as the first downstream CAG trinucleotide (16). The factors that determine how these potential branch points are utilized in the

mouse *GGT* gene are not yet known. The presence of these intron sequences in a human *GGT* gene together with their regulation in a developmental-stage and tissue-specific fashion in the mouse *GGT* gene suggests that they serve a common role in *GGT* gene expression in these two species. Determination of the degree of conservation will require further examination of the *GGT* genes of additional species such as the rat, the dog, the pig, and the cow. But these sequences are not found in the *GGT* gene(s) of bacteria, yeast, flies, or worms, suggesting that they are a relatively late addition to the genomes of metazoans. Further studies will be required to fully understand the complete role of these intron sequences for *GGT* gene expression. However, we note that the identical intron sequences are also found in the human lung-specific group II GGT cDNAs where they reside not in the coding domain but in the 5′-untranslated region (11). Similar, but not identical, sequences are also present in a human intronic GGT promoter (21).

Our PCR data on the relative expression of GGTΔ7 indicate that this alternative splicing event is minor compared with the constitutive event. However, we also found that the GGTΔ7 splicing variant was detectable in tissues where constitutive GGT mRNA was highly expressed, like the kidney, but not in tissues where GGT mRNA abundance is very low, like the liver. Hence, the expression of constitutive GGT and GGTΔ7 appears to be linked. An alternative splicing event like GGTΔ7 has previously been described in a human GGT mRNA, but three potential protein products were predicted based on the presence of different open reading frames (4). Our study in the mouse is the first to characterize the encoded protein product. Our characterization of GGTΔ7 expression in stable and transiently transfected CHO cells reveals that a single truncated form of GGT protein is synthesized. It is a glycoprotein of 44 kDa and has 14 novel residues at the C terminus. It is a relatively stable protein with a half-life of ~8 h and is localized to the ER rather than the cell surface. Because it lacks the C-terminal small subunit residues of the active site, it predictably has no transferase activity. However, it does retain the critical arginine 107 for substrate binding (23). Because recent studies have established an essential role for the GGT substrate glutathione in regulating the redox state of the ER (24), it is possible that GGTΔ7 can bind glutathione and acts as a sensor for glutathione levels within this compartment. Alternatively, the GGTΔ7 isoform may act as a chaperone for the synthesis of the native enzymatically active GGT, blocking its activity within the ER where degradation of glutathione would be unwanted. This would be supported by finding that GGTΔ7 predominantly exists in tissues where high levels of GGT are synthesized, and the low level of GGTΔ7 would reflect that amount needed to balance the low transient levels of newly synthesized native GGT in the ER.

The dinucleotides delimiting the possible alternative 5′- and 3′-splice sites in GGTΔ2–5 and GGTΔ8–9 differ from the consensus GT and AG sequences. Hence, it is unclear exactly how these alternative events were processed but there are certainly many examples in other genes of splice sites that differ from the GT-AG consensus (25), including the human *GGT* genes (22). The presence of such sites led to the recent search and identification of an alternative intron subclass that is bounded by AT-AC dinucleotides. Therefore, other intron subclasses may also occur (26). Until further information becomes available in this area, the mechanism for these alternative splicing events in mouse GGT will remain uncertain. Nonetheless, the similarities between the developmental-stage and tissue-specific expression of GGTΔ8–9 and GGTΔ7 suggests that these GGT mRNA splicing events are highly regulated, whereas the differences in tissue-specific expression suggest they can be regulated independently. We were not able to find a human correlate for GGTΔ8–9, so this event may be specific to the mouse. The protein isoforms derived from GGTΔ2–5 and GGTΔ8–9 lack γ-glutamyltransferase activity, like GGTΔ7. In each case, a residue required for GGT activity, glutamic acid 108 (23) and aspartic acid 423 (27), respectively, is eliminated along with several other amino acids. GGTΔ2–5 and Δ8–9 were also localized to the ER. Coexpression studies failed to show any effect of these isoforms, including GGTΔ7, on total endogenous GGT activity or delivery of active transferase to the cell surface (data not shown). Hence, their exact function remains obscure. Certainly the more rapid turnover rates for Δ2–5 and Δ8–9 could indicate that these glycoproteins are sensed as abnormal GGT products within the ER and targeted for degradation.

Nonetheless, the expression of GGTΔ1 and GGTΔ7 protein isoforms appears to be able to impact the environment of the ER as suggested by their ability to trigger an ER stress response with a change in cell culture conditions. This stress was demonstrated by the parallel induction of the mRNAs for CHOP, a nuclear protein that is regulated by ER stress, and BiP, a chaperone whose expression during ER stress is coordinately regulated with CHOP (28). The message for CHOP is not normally expressed in cells but is strongly induced by ER stress. CHOP protein then forms stable heterodimers with C/EBP family members and binds to novel DNA target sequences to alter the pattern of cellular gene expression in response to ER stress. When the ER stress is severe, CHOP can activate a programmed cell death pathway. The ability to trigger this response appears to be limited to the full-length mouse GGT protein and the truncated GGTΔ7 protein isoform under the conditions tested here. But the change in cellular phenotype as well as the level of induction of CHOP mRNA was dramatic in these two cell lines. CHOP can be strongly induced by deprivation of nutrients such as glucose as well as the amino acids arginine, leucine, lysine, methionine, phenylalanine, and threonine, but none of these molecules were limiting in our conditions (29). However, reduced Cys is found in Ham's F-12 and not in DMEM, which has only oxidized Cys, and this could directly impact the redox state of the ER. The lack of CHOP induction in two other stably transfected CHO cells lines overexpressing human glycoproteins hCAR or hMUC1 suggests that this triggering effect may be specific for these GGT isoforms. Further study will be required to understand the basis for the ER stress and the outcome of CHOP induction in these cell lines, but this will provide new insight into a role for GGT and its isoforms in this intracellular compartment. In addition, the $GGT^{enu1}$ mouse, an animal model of oxidant stress due to GGT deficiency, allows one to study how the loss of GGT enzyme activity affects the pattern of GGT mRNA splicing. In preliminary experiments, we found that the GGTΔ7 splicing event is increased in the lung of these animals, further supporting a connection between GGT activity and the Δ7 splicing event. The common expression of this event in human GGT suggests that the results of further studies on mouse GGT will be directly relevant to our understanding of human *GGT* gene expression and ultimately the role of GGT in mammalian cellular physiology and glutathione metabolism.

*Acknowledgments*—We acknowledge Dr. Ora Weisz and Jennifer Henkel for assistance with immunofluorescence microscopy of the COS-transfected cells, and Carol L. Kinlough, Paul A. Poland, James B. Bruns, and Yue Liu for technical assistance.

REFERENCES

1. Shi, Z.-Z., Habib, G. M., Lebovitz, R. M., and Lieberman, M. W. (1995) *Gene.* **167,** 233–237
2. Curthoys, N. P. (1992) in *Glutathione: Metabolism and Physiological Functions* (Vina, J., ed) pp. 217–225, CRC Press, Boca Raton, FL

3. Sakamuro, D., Yamazoe, M., Matsuda, Y., Kangawa, K., Taniguchi, N., Matsuo, H., Yoshikawa, H., and Ogasawara, N. (1988) *Gene.* **73,** 1–9
4. Pawlak, A., Cohen, E. H., Octave, J., Schweickhardt, R., Wu, S., Bulle, F., Chikhi, N., Baik, J., Siegrist, S., and Guellaen, G. (1990) *J. Biol. Chem.* **265,** 3256–3262
5. Jean, J. C., Harding, C. O., Oakes, S. M., Yu, Q., Held, P. K., and Joyce-Brady, M. (1999) *Mutagenesis* **14,** 31–36
6. Ramsey-Ewing, A., and Moss, B. (1996) *J. Biol. Chem.* **271,** 16962–16966
7. Weisz, O. A., and Machamer, C. E. (1994) *Methods Cell Biol.* **43,** 137–159
8. Gottardi, C. J., and Caplan, M. J. (1992) *J. Tissue Cult. Methods* **14,** 173–180
9. Capraro, M. A., and Hughey, R. P. (1983) *FEBS Lett.* **157,** 139–143
10. Hughey, R. P., and Curthoys, N. P. (1976) *J. Biol. Chem.* **251,** 7863–7870
11. Wetmore, L. A., Gerard, C., and Drazen, J. M. (1993) *Proc. Natl. Acad. Sci. U. S. A.* **90,** 7461–7465
12. Altschuler, Y., Kinlough, C. L., Poland, P. A., Bruns, J. B., Apodaca, G., Weisz, O. A., and Hughey, R. P. (2000) *Mol. Biol. Cell* **11,** 819–831
13. Bergelson, J. M., Cunningham, J. A., Droguett, G., Kurt-Jones, E. A., Krithivas, A., Hong, J. S., Horwitz, M. S., Crowell, R. L., and Finberg, R. W. (1997) *Science* **275,** 1320–1323
14. Breitbart, R. E., Andreadis, A., and Nadal-Ginard, B. (1987) *Ann. Rev. Biochem.* **56,** 467–495
15. Rajagopalan, S., Wan, D.-F., Habib, G. M., Sepulveda, A. R., McLeod, M. R., Lebovitz, R. M., and Lieberman, M. W. (1993) *Proc. Natl. Acad. Sci. U. S. A.* **90,** 6179–6183
16. Smith, C. W. J., Chu, T. T., and Nadal-Ginard, B. (1993) *Mol. Cell Biol.* **13,** 4939–4952
17. Laperche, Y., Guellaen, G., Barouki, R., and Hanoune, J. (1992) in *Glutathione: Metabolism and Physiological Functions* (Vina, J., ed) pp. 79–92, CRC Press, Boca Raton, FL
18. Drozdz, R., Parmentier, C., Hachad, H., Leroy, P., Siest, G., and Wellman, M. (1998) *Free Radic. Biol. Med.* **25,** 786–792
19. Karinch, A. M., and Floros, J. (1995) *Am. J. Respir. Cell Mol. Biol.* **12,** 77–88
20. Karinch, A. M., and Floros, J. (1995) *Biochem. J.* **307,** 327–330
21. Leh, H., Courtay, C., Gerardin, P., Wellman, M., Siest, G., and Visvikis, A. (1996) *FEBS Lett.* **394,** 258–262
22. Courtay, C., Heisterkamp, N., Siest, G., and Groffen, J. (1994) *Biochem. J.* **297,** 503–508
23. Ikeda, I., Fujii, J., and Taniguchi, N. (1993) *J. Biol. Chem.* **268,** 3980–3985
24. Hwang, C., Sinskey, A. J., and Lodish, H. F. (1992) *Science* **257,** 1496–1502
25. Dietrich, R. C., Incorvaia, R., and Padgett, R. A. (1997) *Mol. Cell.* **1,** 151–160
26. Tarn, W.-Y., and Steitz, J. A. (1997) *Trends Biochem. Sci.* **22,** 132–137
27. Ikeda, Y., Fujii, J., Taniguchi, N., and Meister, A. (1995) *J. Biol. Chem.* **270,** 12471–12475
28. Zinszner, H., Kuroda, M., Wang, X., Batchvarova, N., Lightfoot, R. T., Remotti, H., Stevens, J. L., and Ron, D. (1998) *Genes Dev.* **12,** 982–995
29. Bruhat, A., Jousse, C., Wang, X.-Z., Ron, D., Ferrara, M., and Fafournoux, P. (1997) *J. Biol. Chem.* **272,** 17588–17593